Available online at www.sciencedirect.com
ScienceDirect
International Journal of Impact Engineering 33 (2006) 723–734
INTERNATIONAL JOURNAL OF IMPACT ENGINEERING
www.elsevier.com/locate/ijimpeng

Influence of impact velocity on fragmentation and the energy efficiency of comminution

S. Sadrai[a,*], J.A. Meech[a], M. Ghomshei[a], F. Sassani[b], D. Tromans[c]

[a]*Department of Mining Engineering, The University of British Columbia, Vancouver, BC, Canada V6T 1Z4*
[b]*Mechanical Engineering, The University of British Columbia, Vancouver, BC, Canada V6T 1Z4*
[c]*Materials Engineering, The University of British Columbia, Vancouver, BC, Canada V6T 1Z4*

Available online 15 November 2006

Abstract

Comminution processes such as crushing and grinding are essential stages in mining and mineral processing operations to reduce the size of ore and rock, and to liberate the valuable mineral for beneficiation. Comminution is energy-intensive and responsible for most of the energy used during mineral recovery. Energy efficiency is very low since almost all the energy is dissipated as heat instead of generating new surface area. This paper reports on studies conducted on strain rates achieved by various velocities of impacts that enhance energy efficiency and mineral liberation. The research focuses on understanding comminution fracture mechanics and on quantifying the distribution of energy with respect to generating new surface area. In interpreting breakage energy phenomena, accurate measurements of surface roughness and surface area are essential. A novel approach to measure surface roughness and surface area based on a fractal analysis procedure has been developed. Changes in surface roughness of broken specimens under variable loading rates were studied using a laser probe to generate 3D topographical maps of the fracture surfaces. The results indicate that surface roughness and hence, specific surface area, increase with increasing loading rate by several orders of magnitude as particle size decreases to ~1 μm. Below this limit, surface roughness begins to diminish from particle–particle attrition. An apparatus to measure the quantitative parameters of impact at different velocities on aggregated rock samples is proposed. Experiments are being carried out at projectile velocities up to 500 m s^{-1} utilizing a compressed-air device. The results suggest possible efficiency improvements in breakage under the velocity of impact.

Keywords: Comminution; Energy efficiency; Impact velocity

1. Introduction

During the last decade, as competition has intensified in the world mining industry, mining operations continuously pursue lower operating costs. Comminution costs represent an important contribution, 30–50%, of total mining operating costs [1]. It has been reported that about 3% of world electrical energy is consumed by comminution [2] while in the US about 1.3% of the electrical energy is consumed by comminution [3].

*Corresponding author. Tel.: 00 + 1 604 822 4642; fax: 00 + 1 604 822 5599.
E-mail address: sepehr@mining.ubc.ca (S. Sadrai).

0734-743X/$ - see front matter © 2006 Elsevier Ltd. All rights reserved.
doi:10.1016/j.ijimpeng.2006.09.063

Thus, every aspect of comminution justifies careful consideration in order to minimize all elements of cost and associated energy use.

Crushing and grinding are essential components of all mining and mineral processing operations to reduce the size of ore and rock, and subsequently, liberate the valuable mineral for beneficiation. However, comminution is very energy-intensive and consumes a major percentage of the total energy used during mineral recovery. In many cases, the efficiency of comminution is derived by measuring the ratio of energy "required" to energy used. From a fundamental viewpoint, it is the energy required to create new surfaces that should be considered (see Fig. 1).

Using this definition, comminution has been shown to be of the order of 1–2% efficient [4–6]. Typical grinding efficiencies range from 1% to 2% with crushing efficiencies lying slightly higher at 3–4%. High-pressure rolls and roller crushers are reported to operate at levels as high as 7–8%, while blasting shows the highest efficiency of all processes ranging from 13% to 20%. Most of the energy input into comminution ends up as heat generated within the rock material, equipment, and water to eventually be dissipated into the surrounding atmosphere. Fig. 2 shows a recent example of measurements on a large ball mill [7].

Surface area of fractured material is an important measurement to characterize energy use in comminution as well as surface reactions in down-stream processing steps. Conventional approaches to direct measurement of surface area consider the geometry of product and feed particles—both size and shape. What is often overlooked in such work is the influence of fractal geometry factors-surface roughness and the resolution used to measure roughness. Parameters that characterize surface variations include roughness and waviness, which

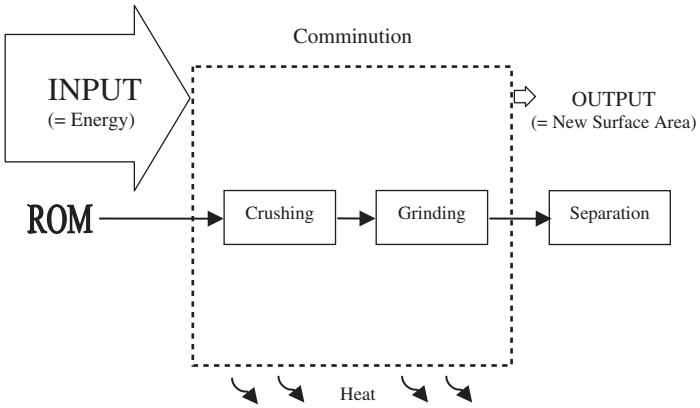

Fig. 1. Comminution inefficiency.

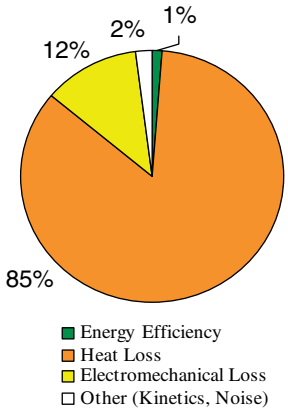

Fig. 2. Energy distribution during comminution process.

are dimensional properties of the material. Roughness is defined as relatively finely spaced surface irregularities, of which the height, width, and direction establish a definite surface pattern. Waviness refers to a wavelike variation from a perfect surface to one with much wider spacing and higher amplitude changes than surface roughness [8].

One way to analyze the fracture of materials is to determine the topography of a fractured surface. Fracture surfaces have different degrees of roughness and therefore geometrical complexity is a characteristic measure [9]. In order to distinguish between different surfaces, the roughness can be expressed as a mathematical relation [10].

The use of "fractal dimension" is a way to estimate surface roughness independent of conventional statistical analysis [11]. Fractal analyses of rock surfaces include a variety of one and two-dimensional techniques. Each method provides a consistent means to generate essential information to designate roughness. As such, fractal parameters can be a valuable tool in evaluating rock properties [12].

The aim of this study was to investigate the influence of different loading rates or strain rates in both static and dynamic regimes on rock fragmentation. A coefficient of surface roughness was developed as an index to calculate the true surface area of broken samples. To achieve this goal a laser probe was used to obtain a digital data set that represented the fracture surface.

2. Experimental procedure

In order to measure the efficiency of breakage, four drill core samples of volcanic rock (tuff) from Northern Ontario with diameters of about 47 mm and aspect ratios between 2.5 and 3 were prepared and polished flat at the two-end surfaces. Compressive tests under different loading rates were conducted using a static compressive testing machine (MTS) and stress-versus-strain curves were plotted. Applied loading rates were 10, 20, 30, and 100 $\mathrm{kN\,min^{-1}}$, respectively. Unlike the general agreement, it was noticed that the peak stress decreased with increasing loading rate due to the rock sample inhomogeneity and porosity.

2.1. 3D mapping

A laser profilometer (National Research Council of Canada—NRC) was used to study the surface roughness of the broken rock [8]. This is a non-contact device able to produce a datafile of x, y, and z coordinates. The profilometer consists of a laser probe mounted on a coordinate measuring machine. The probe automatically moves over the sample to measure the topography of the fracture surface. Data are collected and processed using a personal computer.

As shown in Fig. 3, topographical measurement of the fracture surface was carried out with a 3D imaging program (Mapping—developed by NRC) and an isometric view of the entire scanning field was constructed. The coarsest piece of the broken parts in each test was chosen and sample positions were selected in a direction such that the laser beam scanned parallel to the application of the compressive force. The scanning field was 10×10 mm.

In addition, imaging software enabled us to create cross-section profiles of the entire surface. The distance between profiles in sequence is a constant dependent on the scanning interval (resolution). For our experiments, the probe provided a resolution of either 62.5 or 30 μm. In this way, a one-dimensional shape of each surface profile was obtained (Fig. 4).

The sample traces are cross-sections perpendicular to the surface plane in the "x" direction, i.e., parallel to the application of the compressive force. A large number of traces (150–350) for each sample were performed. A computer program, EASYDIG, facilitated the digitization and measurement of the surface topography along each trace.

2.2. Development of surface roughness technique

Considering the scale of each plot, the roughness factor can be defined as the ratio of the length of the surface topography to the width of the trace (as a reference) in that cross section.

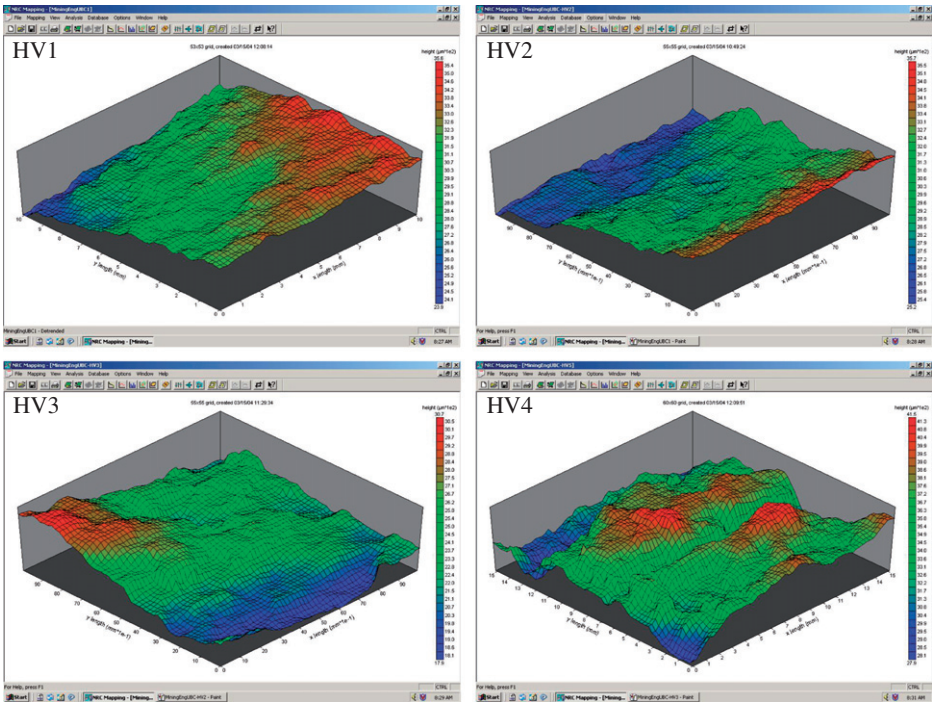

Fig. 3. Surface topography of the rock fracture measured by the laser probe.

The results of these measurements are graphed for each sample in Fig. 5. The ranges of roughness factors are compared in Fig. 6, indicating that the sample with the highest loading rate exhibits the roughest surface. The mean value is the "roughness factor" in one direction. For surface calculation, the results obtained for one direction can be extended into the second direction since the grid cells have equal length in both directions and the loading force acts in shear along the sample. So, the "surface factor" is found by squaring the roughness factor to provide a 2D measure (see Table 1). The results indicate that roughness factor increases about 40% in one direction and about 100% in two directions with an order of magnitude increase in loading rate.

Fig. 7 summarizes these results with the trend line showing the enhancement of roughness and surface factor as loading rate increases. As well, note the steady increase in the range (S.D.) of results as a function of loading rate indicating breakage becomes increasingly heuristic at high loading rates.

2.3. Development of surface area technique

Next, it is necessary to find the new surface area created by breakage. Three methods have been developed to obtain the produced surface area based on particle size analysis. A Quantachrome surface area analyzer (BET) was used to measure the surface area of the finest particles ($<400\,\mu m$). For coarse particles between 400 μm and 9.5 mm, surface area was estimated theoretically using the arithmetic mean size of each fraction [13] assuming cubic particles (Fig. 8a) together with an estimate of the shape factor for each fraction. For the coarsest sizes (>9.5 mm), the exact shape of each piece can be readily determined and so, direct measurement of the surface of each piece was done by rolling on a piece of paper and outlining the extreme boundaries (Fig. 8b).

So it is possible to measure and/or calculate the apparent specific surface area of the total broken material from each test. In applying shape factors (1.0–1.6), changes in this parameter as a function of particle size was considered to be linear. Gaudin [13] recommended a shape factor of 1.75 for finest particles for Quartz in practice. Obviously this assumption requires more detailed study to establish how the parameter size-relationship changes for different materials and/or environments.

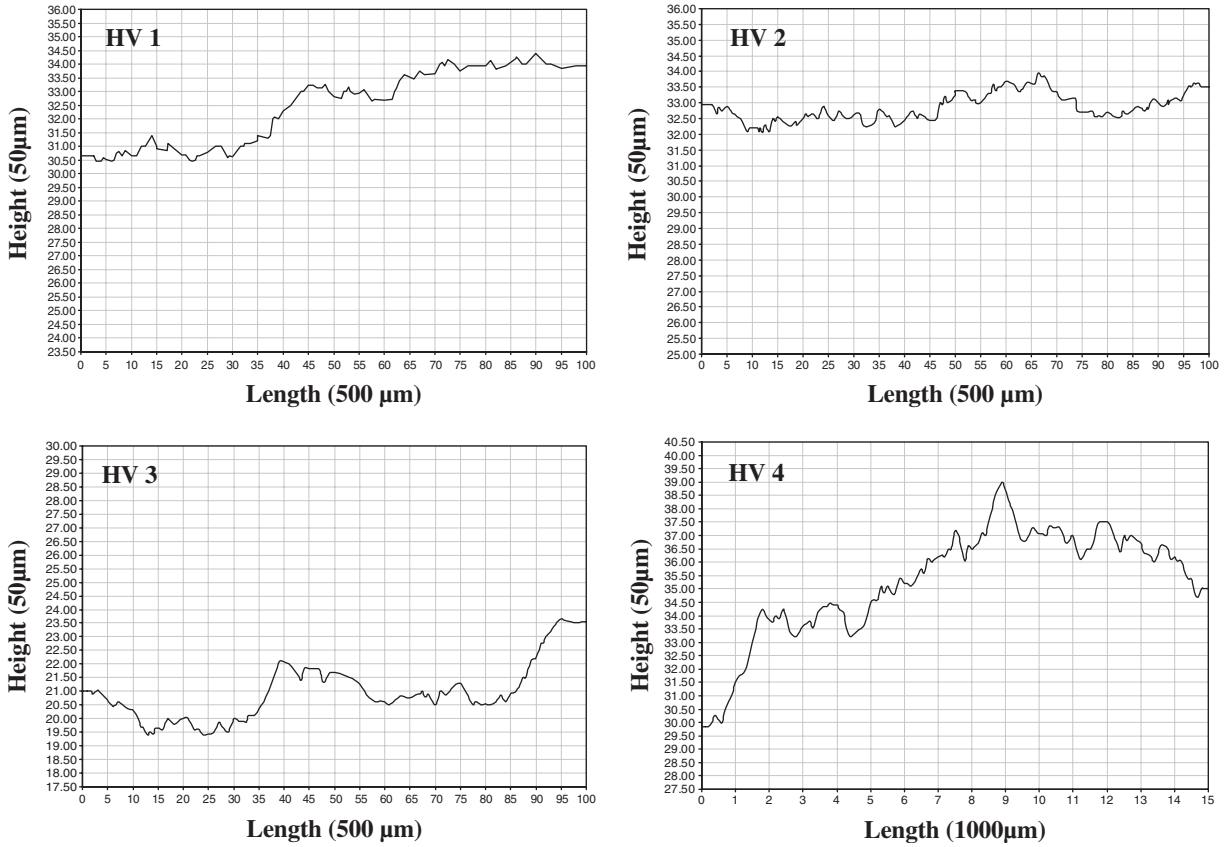

Fig. 4. Examples of the trace profile in the "x" direction.

For surface roughness as a function of particle size, it was necessary to combine directly measured surface roughness of coarse particles (measured at a resolution of 30–60 µm) with the B.E.T. measurements for the finest sizes measured at a resolution of 4 Å (i.e., the diameter of nitrogen atoms adsorbed during B.E.T. measurement). So the data for surface roughness of the coarsest sizes shown in Table 1 were adjusted to a resolution of 4 Å by applying a factor determined from the B.E.T. surface area measurement and the expected surface area based on mean particle size. Fig. 8c depicts our anticipated surface roughness-particle size relationship for all samples tested.

Note that a decline in surface roughness occurs for the B.E.T. estimates for the finest two sizes (210 and 710 µm). We believe that this drop is an actual physical occurrence and that surface roughness will continually decline in comminution as particle size decrease below 1 µm. Surface roughness is reduced as edges and kinks on the surfaces of ultra-fine particles are worn away by attrition as particle size declines to the size of the crystal lattice [14].

Based on this technique (measurement, calculation, and theory), the ultimate specific surface area and total surface area for each fraction was obtained (see Table 2). It can be seen that almost half of the new surface area was produced on the finest particles, which makes up only ~0.2% by weight of the total sample. So, half of the newly created surface area occurred within less than 1 g of the total sample. Clearly, material loss during a test can significantly affect the accuracy of measuring new surfaces (recovery of minute dust particles is extremely important to ensure surface areas are determined accurately). Overall accuracy of surface area depends on several parameters such as shape factor estimation, weight measurement of each size fraction, assumptions inherent in a B.E.T. measurement, material porosity, and measurement resolution.

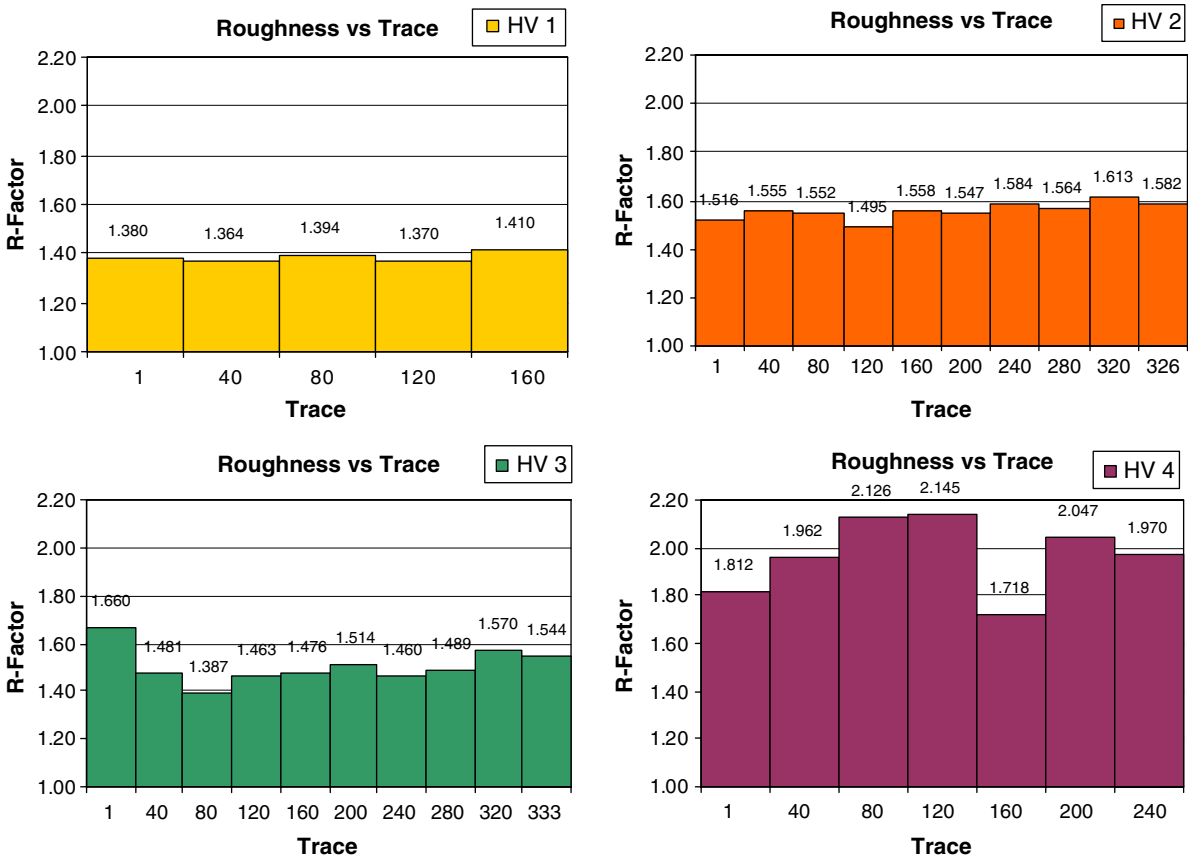

Fig. 5. Roughness factor measurements along traces.

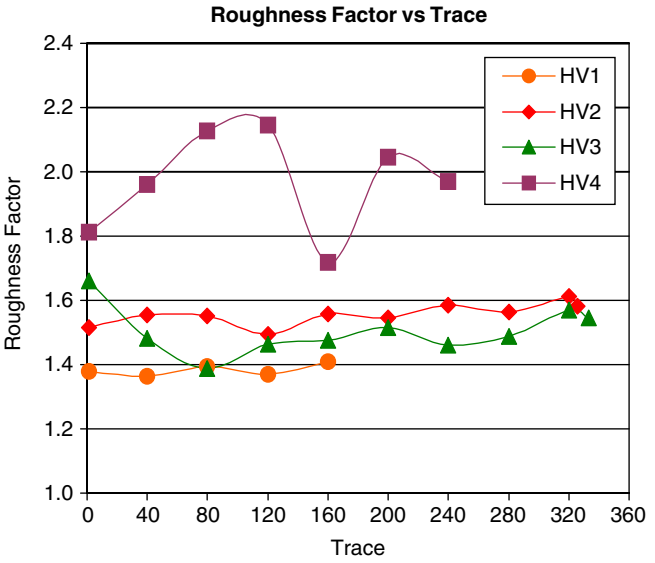

Fig. 6. Comparison of roughness factor along the traces.

Table 1
Coefficient of surface and roughness factor

Sample	Roughness factor	S.D.	Surface factor
HV1	1.384	0.019	1.92
HV2	1.557	0.034	2.42
HV3	1.504	0.074	2.26
HV4	1.969	0.158	3.88

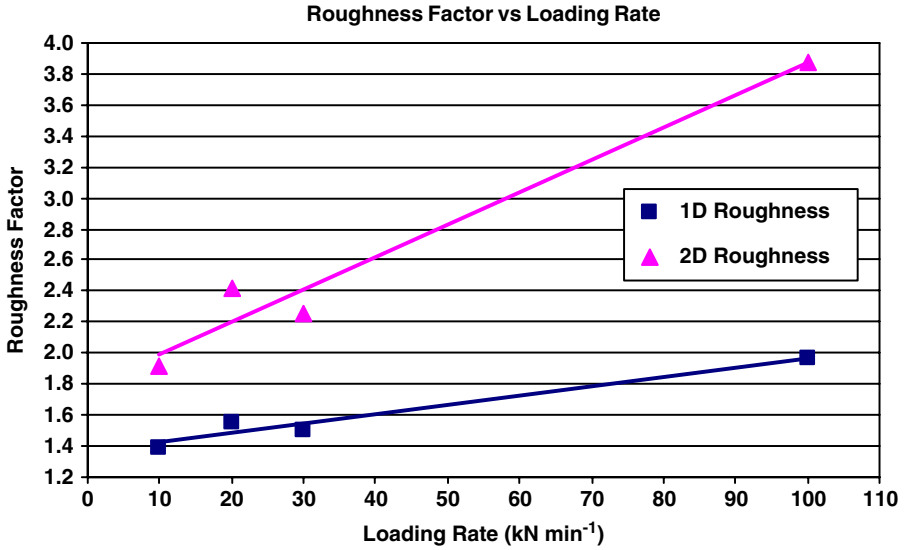

Fig. 7. Roughness and surface factor vs. loading rate.

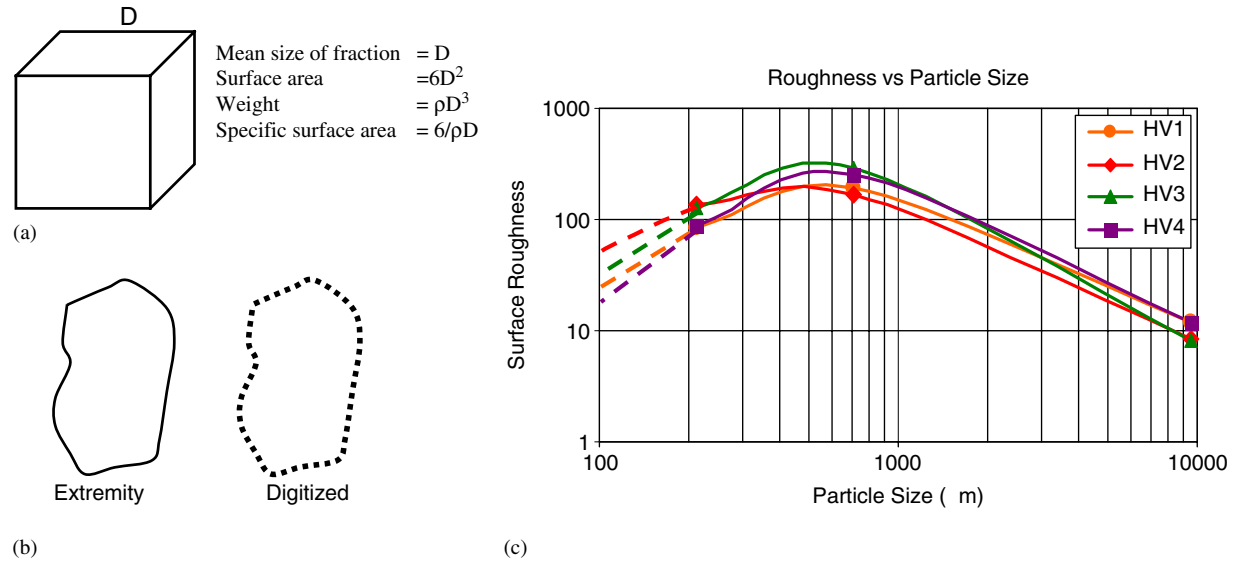

Fig. 8. (a) Theoretical calculation of specific surface area; (b) direct measurement of the specific surface area of the coarsest pieces; and (c) estimation of surface roughness as a function of particle size for a measurement resolution of 4 Å.

Table 2
Estimation of surface area based on theory, measurement and calculation

Fraction (mm)	HV1		HV2		HV3		HV4	
	Ultimate SSA (cm^2/g)	Surface area (%)	Ultimate SSA (cm^2/g)	Surface area (%)	Ultimate SSA (cm^2/g)	Surface area (%)	Ultimate SSA (cm^2/g)	Surface area (%)
+9.52	12.58	27.37	8.12	10.10	10.79	17.49	10.03	38.19
+4.76	59.53	2.76	49.57	2.51	48.77	3.62	59.81	2.29
+2.38	196.71	6.28	192.57	4.43	187.69	4.64	198.57	3.92
+1.00	679.69	8.88	782.18	8.30	755.38	8.94	689.33	9.20
+0.42	2624.45	11.46	3550.30	13.94	3397.29	14.30	2674.21	12.42
+0.00	14293.87	43.25	22730.44	60.72	21551.71	51.02	14633.50	33.98
Total	43.96	100.00	74.92	100.00	57.52	100.00	25.73	100.00

(SSA = Specific surface area)

Table 3
Estimation of produced surface area of breakage in an MTS machine

Sample	Loading rate (kN/min)	Diameter (cm)	Length (cm)	Initial surface area (cm^2)[a]	Modified initial surface area (cm^2)[b]	Determined final surface area (cm^2)	Produced surface area (cm^2)
HV1	10	4.745	13.592	237.98	290.34	29082.07	28791.73
HV2	20	4.746	13.591	238.02	290.39	50161.12	49870.73
HV3	30	4.745	13.564	237.56	289.83	38019.90	37730.08
HV4	100	4.746	13.668	239.17	291.79	17228.47	16936.68

[a]Outer surface area of core samples before breakage.
[b]Projection of initial surface area based on the resolution of measurement at 4 Å.

Table 4
Estimation of energy and power efficiency of breakage in an MTS machine

Sample	Surface energy (J)	Maximum force (KN)	Maximum displacement (mm)	Consumed energy (J)	Energy efficiency (%)	Time (s)	Power efficiency (%/s)
HV1	5.76	247.31	0.7768	96.05	5.99	1480.83	0.0040
HV2	9.97	233.53	0.7289	85.11	11.72	703.78	0.0167
HV3	7.55	224.29	0.8431	94.55	7.98	452.88	0.0176
HV4	3.39	172.99	0.6230	53.89	6.29	116.29	0.0541

2.4. Energy efficiency

As shown above, a method exists to calculate the surface area after breakage and the change in surface area can be obtained. So, it was possible to determine how much energy was expended to create new surface area assuming the specific surface energy of the rock is equal to that of quartz, i.e., 2000 erg cm^{-2} [3]. The amount of energy input into the rock core during a test can be determined to calculate the efficiency of breakage. Tables 3 and 4, and Fig. 9 present the results of this analysis.

As expected, the trend in energy efficiency was slightly decreased or almost constant because the tests were performed in a static regime with low strain rate. However, the power efficiency was significantly improved as loading rate increased. That is, the energy was consumed in shorter times at higher loading rates resulting in better use of power to create new surfaces.

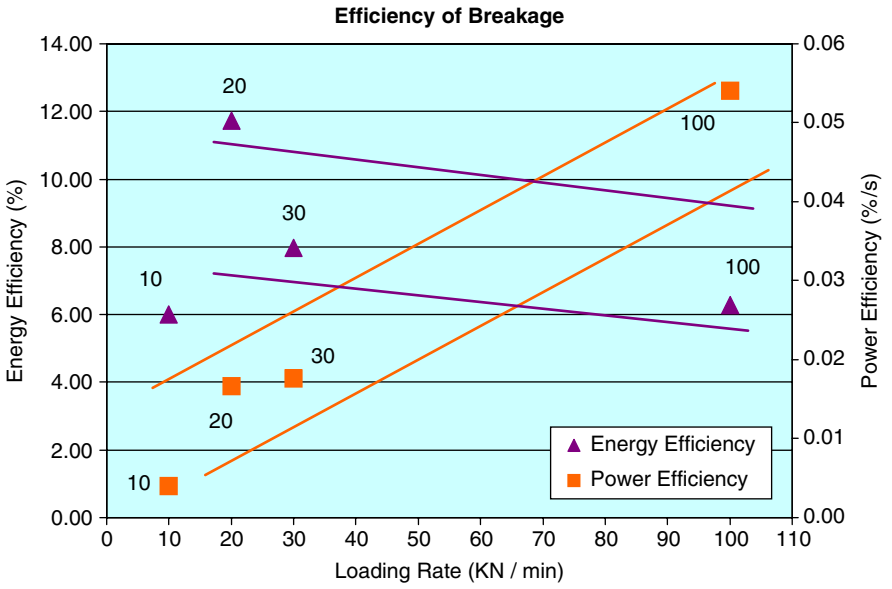

Fig. 9. Energy efficiency of breakage and power efficiency.

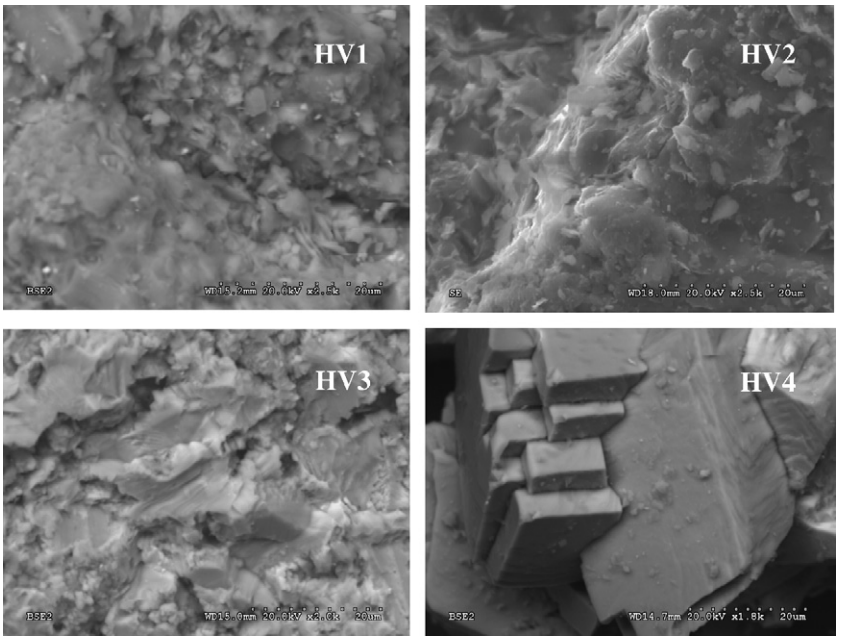

Fig. 10. SEM examinations of the samples.

2.5. SEM examinations

Scanning electron microscopy (SEM) was used to examine the breakage phenomenon of the ultra-fine particles. It was observed that a considerable amount of fine macro-sized steps or spikes were present on the coarsest particle faces. Also, the existence of numerous surface cracks (fissures) was apparent. HV4 (the highest loading rate) actually revealed this breakage pattern at the dimensions of the crystal structure (Fig. 10).

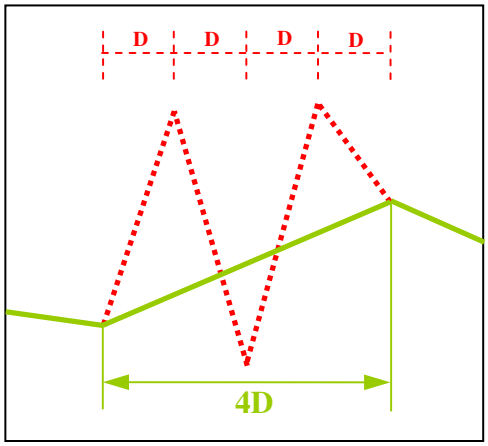

Fig. 11. Effect of resolution on roughness and surface area measurement.

3. Effect of resolution on roughness and surface area measurement

This study identifies that the measurement of surface area is highly dependent on the measurement resolution. Different values of surface area result when the resolution is changed. So the meaning of surface area in terms of the objective of a study is an important aspect in choosing the resolution to use in the measurement technique. The less dense the network of the grid, the less accurate the individual cells are reflected, and the lower will be the measured surface area. The surface profile shown in Fig. 11 indicates the influence of resolution on the roughness measurement and ultimately, on surface area. With D as the resolution instead of $4D$, the measured surface area increases by 2–3 times. In order to interpret breakage phenomena, it is clear that the essential accuracy requires measurements at the dimensions of the crystal lattice since breakage takes place with the breaking of bonds between elements in the crystal lattice.

4. Higher-velocity impact comminution

Impact velocities in most comminution equipment is about $10\,m\,s^{-1}$ while in blasting, the impact produces shock waves in all directions that move through the rock with velocities of $2\,km\,s^{-1}$ or greater [15–16]. In order to study comminution in this higher velocity regime [17–20], an apparatus to measure the quantitative parameters of impact velocity on aggregated rock samples has been developed. Experiments are being carried out at projectile velocities from 5 to $500\,m\,s^{-1}$ using a compressed-air device. The results suggest possible efficiency improvements in breakage under the velocity of impact.

Conventional high-strain-rate, high-velocity impact facilities [21] are used to attempt to improve the strength of materials subjected to high energy inputs. Our research at UBC-CERM3 is using this approach instead to improve on fragmentation methods and minimize energy use during comminution.

4.1. Design basis

Fig. 12 illustrates the UBC-CERM3 facility to conduct the impact velocity experiments. The apparatus consists of a reservoir, a launch-tube, a target chamber, flanges, supports, and structure. The reservoir acts to accumulate a measured quantity of high-pressure air. Before each test, the reservoir is charged to the desired pressure using a compressor. The reservoir, launch tube, and striker constitute a unified system able to convert potential energy into kinetic energy. Thus, a relationship among pressure, volume, velocity, and mass can be obtained by equating the potential energy of the gas to the striker's kinetic energy [22]. As a first approximation, it is assumed that the air behaves as a perfect gas with adiabatic expansion. As well, loss in transferring energy from the gas to the striker is assumed to be negligible. In actuality, a small amount of this energy is converted to heat. The reservoir is designed with sufficient capacity to accelerate the projectile to a

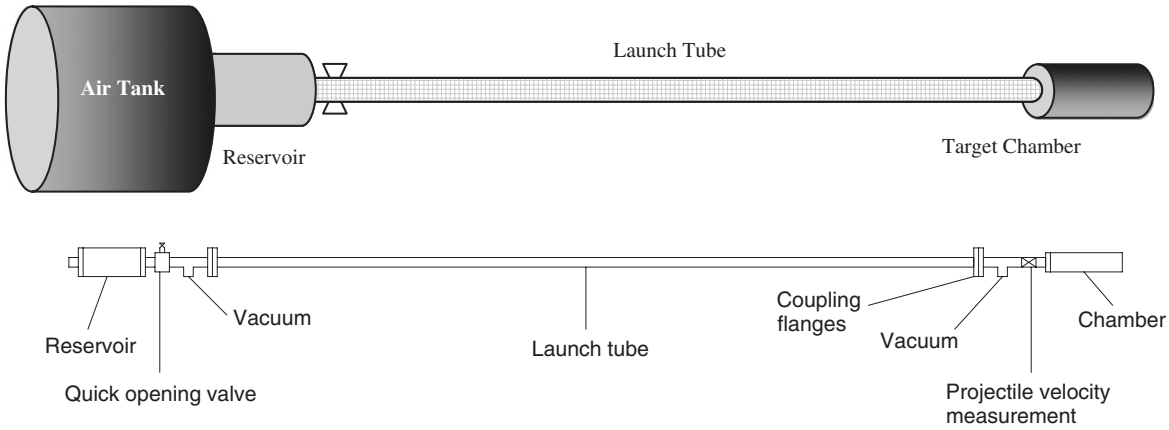

Fig. 12. UBC-CERM3 high-velocity-impact comminution apparatus.

velocity of $500\,m\,s^{-1}$. Different projectile masses and diameters were examined to select a suitable inside diameter for the tube. Based on these analyses, a maximum pressure of 2 MPa (300 psi) is necessary. This pressure is considered to generate the critical stress for design purposes, although, in reality the energy will distribute throughout the system at a lower pressure. All sections of the machine are made from mild steel with tensile and shear strengths of about 300 and 100 Mpa, respectively. For overall safety, a material factor of safety of 1.5 was chosen. The air gun can launch a projectile of high-strain-rate steel or aluminum-alloy. The projectile velocity immediately before impact is measured by two pairs of laser diode detectors.

This apparatus is a one-of-a kind machine to measure the effect of high-strain-rates on rock breakage. Bulk material samples are tested rather than single rock particles in order to provide void space for expansion of the smaller broken particles. Compressed air is cheap, clean, and relatively safe as a generating force. A novel cylinder and piston design is incorporated in the apparatus compatible with both high pressure and velocity.

5. Discussion and recommendations

In this study, the surface roughness of four volcanic rock samples was investigated under different loading conditions. A representative area was selected to be measured in each sample. With increasing loading rate, the roughness factor in one direction and surface factor in two directions increase resulting in greater enhancement in surface area production. However, conventional measurement of surface area of broken material is fraught with considerable error due to lack of accounting for surface roughness. As well, surface roughness measurements depend on the resolution used to make the measurement. Volcanic rocks such as tuff are highly porous which can affect the calculation of surface area and estimation of energy efficiency. We intend to carry out similar tests for other types of rocks and minerals such as halite, limestone, and granite that possess coarse crystal sizes and low porosity and micro-fracture densities.

From the above considerations, it appears that the application of different loading rates or the use of various impact velocities and strain rates may provide an opportunity to achieve improved economies in rock breakage.

6. Conclusions

1. True energy efficiency appears to be higher than previous estimations (i.e., 5–10% instead of 1–2% for the Tuff samples) but this must be verified with rock samples that possess low porosity and micro-fracture densities.
2. Surface area measurement depends on the resolution of measurement. For meaningful results consideration of the utility of the data is important in deciding on the resolution required.
3. A low estimate of the surface area produced in a comminution test is obtained unless very close experimental control of dust collection is used.

4. The surface roughness factor plays an important role in determining the energy efficiency of breakage.
5. The implication of impact velocities at higher strain rates than conventional methods as a possible control variable is encouraging for comminution purposes.
6. High roughness factors are due to surface cracks (fissures) and/or fine steps on coarse faceted faces.
7. Almost half of the produced surface area in breaking tuff occurs within the finest particles ($<0.2\%$ by weight).
8. The power or the rate of energy input is likely to result in enhanced surface energy output rate.

References

[1] Radziszewski P. Developing an experimental procedure for charge media wear prediction. J Miner Eng 2000;13(8–9):949–61.
[2] Fuerstenau DW, Lutch JJ, De A. The effect of ball size on the energy efficiency of hybrid high-pressure roll mill/ball mill grinding. J Powder Technol 1999;105(1–3):199–204.
[3] Fuerstenau DW, Abouzeid AZM. The energy efficiency of ball milling in comminution. Int J Miner Process 2002;67(1–4): 161–85.
[4] Tromans D, Meech JA. Fracture toughness and surface energies of minerals. J Miner Eng 2002;15(12):1027–41.
[5] Whittles DN, Kingman SW, Reddish DJ. Application of numerical modeling for prediction of the influence of power density on microwave-assisted breakage. Int J Miner Process 2002;68(1–4):71–91.
[6] Walkiewicz JW, Lindroth DP, Clark AE. Iron ore grindability improved by heating. Eng Min J 1996;197(5):4.
[7] Alvarado S, Alguerno J, Auracher H, Casali A. Exergy-energy optimization of comminution. J Energy 1998;23(2):153–8.
[8] Budinski KG. Engineering materials properties and selection. NJ USA: Prentice Hall; 1989. p. 43–6.
[9] Zhou HW, Xie H. Direct estimation of the fractal dimensions of a fracture surface of rock. J World Sci 2003;10(5):751–62.
[10] Schey JA. Introduction to manufacturing processes. USA: McGraw-Hill Publishing Co; 1987. p. 73–6.
[11] McWilliams PC, Kerkering JC, Miller SM. Estimation of shear strength using fractals as a measure of rock fracture roughness. Report of Investigations, Bureau of Mines, USA, 1993, 36p.
[12] Chakravarty D, Pal SK. Roughness estimation of fractured granite. J Min Met Fuels 1996;44(5):176–81.
[13] Gaudin AM. Principles of mineral dressing. USA: McGraw-Hill Book Company; 1967. p. 124–40.
[14] Tromans D, Meech JA. Enhanced dissolution of minerals: stored energy, amorphism and mechanical activation. J Miner Eng 2001;14(11):1359–77.
[15] Chi G, Fuerstenau MC, Bradt RC, Ghosh A. Improved comminution efficiency through controlled blasting during mining. Int J Miner Process 1996;47(1–2):93–101.
[16] Liu L, Katsabanis PD. Development of a continuum damage model for blasting analysis. Int J Rock Mech Min Sci 1997; 34(2):217–31.
[17] Cho SH, Ogata Y, Kaneko K. Strain-rate dependency of the dynamic tensile strength of rock. Int J Rock Mech Min Sci 2003; 40(5):763–77.
[18] Zhang ZX, Kou SQ, Yu J, Yu Y, Jiang LG, Lindqvist PA. Effects of loading rate on rock fracture. Int J Rock Mech Min Sci 1999;36(5):597–611.
[19] Grady DE. Fragmentation of solids under impulsive stress loading. J Geophys Res 1981;86(B2):1047–54.
[20] Olsson WA. The compressive strength of tuff as a function of strain rate. Int J Rock Mech Min Sci Geomech 1991;28(1):115–8.
[21] Grosch DJ, Riegel JP. Development and optimization of a micro two-stage light gas gun. Int J Impact Eng 1993;14(1–4):3 15–24.
[22] Bourne NK. A 50 mm bore gas gun for dynamic loading of materials and structures. Meas Sci Technol 2003;14(3):273–8.